GEOPHYSICAL RESEARCH LETTERS, VOL. 23, NO. 21, PAGES 2899-2902, OCTOBER 15, 1996

Prediction of magnetic storms by nonlinear models

J. A. Valdivia,[1] A. S. Sharma,[2] and K. Papadopoulos[1,2]

Abstract. The strong correlation between magnetic storms and southward interplanetary magnetic field (IMF) is well known from linear prediction filter studies using the Dst and IMF data. However, the linear filters change significantly from one storm to another and thus are limited in their predicting ability. Previous studies have indicated nonlinearity in the magnetospheric response as the ring current decay rate varies with the Dst value during storms. We present in this letter nonlinear models for the evolution of the Dst based on the OMNI database for 1964-1990. When solar wind data are available in advance, the evolution of storms can be predicted from the Dst and IMF data. Solar wind data, however, are not available most of the time or are available typically an hour or less in advance. Therefore, we have developed nonlinear predictive models based on the Dst data alone. In the absence of solar wind data, these models cannot predict the storm onset, but can predict the storm evolution, and may identify intense storms from moderate ones. The input-output model based on IMF and Dst data, the autonomous model based on Dst alone, and a combination of the two can be used as forecasting tools for space weather.

1. Introduction

The solar wind - magnetosphere coupling is enhanced when the interplanetary magnetic field (IMF), convected by the solar wind to the dayside magnetosphere, is southward. This enhanced coupling energizes the magnetosphere - ionosphere system, leading to an intensified ring current and a magnetic storm. A common measure of storms is the Dst index constructed from the variations of the horizontal component of the magnetic field at 4 mid-latitude ground stations. The intense storms studied in this paper, defined by Dst values below -100 nT, have been identified as the cause of extensive damages to many ground and space based systems, and as such, their understanding is crucial to space weather studies [*Joselyn* , 1995]. Such effects include fluctuating magnetic fields generated on the ground, which can destabilize electric power transmission systems. In space, changes in the magnetosphere can produce energetic particle fluxes that affect satellites, sometimes causing irreparable damage to the electronics on board. Forecasting of magnetic storms is thus an important component of space weather efforts to monitor and predict the near-Earth space environment.

The strong correlation between the Dst and the interplanetary variables during a storm is well known from earlier studies using linear models [*Burton et al.*, 1975]. A typical case of a storm, viz. of 11 February 1981, is shown in Fig. 1. It begins with an increase of the Dst index marking the onset of the storm or the sudden storm commencement, followed by a large decrease during the main phase. The Dst minimum marks the beginning of the recovery phase during which the ring current decays. This phase is not directly correlated to the solar wind induced dawn-to-dusk electric field $E_y = VB_z$, given by the product of the solar wind speed V and the north-south component B_z of the IMF, which recovers on a faster time scale (Fig. 1, top panel).

Many studies of the solar wind – Dst relationship have indicated nonlinearity in the evolution of the Dst [*Burton et al.*, 1975; *Gonzales et al.*, 1994]. For example, *Gonzales et al.*, [1994] report the ring current particle loss rate varied nonlinearly with Dst as follows: $\tau = 4$ hours for $Dst > -50nT$, $\tau = 0.5$ hours for $-50 > Dst > -120$ nT, and $\tau = 0.25$ hours for $Dst < -120$ nT. Also, the linear prediction filters were found to vary from storm to storm [*Sharma et al.*, 1995]. In this letter we develop nonlinear models of magnetic storms using the interplanetary magnetic field and Dst time series data. The Dst index is the most widely used variable that characterizes magnetic storms and has the advantage of having been monitored continuously over many decades. In this paper we use the hourly OMNI data base for the period 1964 - 1990 (available on the NGDC CD-ROM), which has 140 storms with Dst values below -100 nT. The storms are chosen by defining an interval that begins 10 hours before the Dst goes down to -50 nT during the main phase, and ends another 10 hours after the Dst reaches the same value in the recovery phase. Further, the Dst should be persistently above -50 nT during the two 10–hour intervals. The OMNI data base contains only 14 storms with simultaneous measurements of the solar wind variables satisfying this criteria. It is also important to note that even in this relatively large data base we have only a few cases of very large storms (e.g., $Dst < -300$ nT), as shown in Fig. 3. The magnetic field measured at low latitudes is affected significantly by the variations of the solar wind ram pressure $p = nm_+V^2$ which pro-

[1] Department of Physics, University of Maryland, College Park, Maryland.
[2] Department of Astronomy, University of Maryland, College Park, Maryland.

Paper number 96GL02828.
0094-8534/96/96GL-02828$05.00

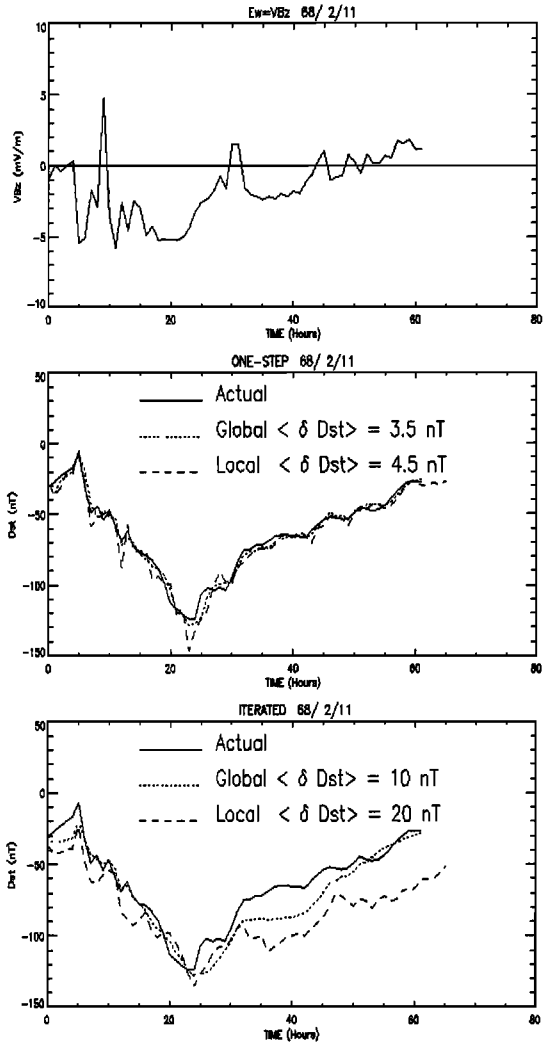

Figure 1. Magnetic storm of 11 February 1968. The solar wind input VBz is shown in the top panel and the actual Dst is shown by the continuous lines in the middle and bottom panels. The one step predictions are shown in the middle panel for the global model given by Eq.(2) (dotted line) and for the local linear technique (dashed line). The iterated predictions starting at t = 1 are shown in bottom panel for the global (dotted line) and local (dashed line) models. The errors for each case are also shown.

duce changes in the magnetopause currents (n is the solar wind density, and m_+ is the proton mass). We follow *Burton et al.*, [1975] and define, when possible, the pressure–corrected $Dst^* = Dst - b\sqrt{p} + c$. For the this OMNI dataset $c = 22$ nT and $b = 10.5nT/(nPa)^{1/2}$.

2. Global Input-Output Model

The time evolution of the ring current, as represented by the Dst index, has been modeled by an input or injection function Q(t) and a recovery with a characteristic time scale τ [*Burton et al.*, 1975], so that

$$\frac{dDst^*(t)}{dt} = Q(t) - \frac{Dst^*(t)}{\tau} = F[\vec{X}(t)], \qquad (1)$$

Many forms of the input function Q(t) have been used [*Gonzales et al.*, 1994], but for our purposes we define the state vector $\vec{X} = [Dst^*, E_w]$, where $E_w = VB_s\sigma_{Dst^*}/\sigma_{VB_s}$ is the normalized solar wind induced electric field, B_s is the southward component of the IMF (zero if B_z is northward), and $\sigma_{VB_s} = 3.7$ mV/m and $\sigma_{Dst^*} = 44$ nT are the standard deviations of VB_s and Dst*, respectively. Taking F in Eq. (1) to be a nonlinear polynomial, the coefficients are obtained from the data of the 14 storms by a fitting procedure based on a predictor-corrector integration scheme [*Brown et al.*, 1994]. This yields

$$\frac{dDst^*}{dt} = -0.08Dst^*[1 - 0.0012Dst^*] + 0.26E_w \qquad (2)$$

with a mean absolute fitting error of 4.5 nT. It describes the evolution of Dst*, and thus the interaction of the solar wind and ring current. The coefficient for Dst^* in the global differential equation (2) corresponds to the inverse of the decay time τ and has a value of $\tau_o \sim$ 12.5 hours, which is consistent with previous studies [see *Gonzales et al.*, 1994]. Comparing Eqs. (1) and (2) we define a Dst^* dependent decay time

$$\tau = \frac{\tau_o}{(1 - 0.0012Dst^*)}.$$

Thus for Dst^* values $\leq -100nT$, the variation of τ due to the nonlinear dependence is significant and intense storms have shorter recovery time scales. Due to the limited number of storms with Dst < -300 nT in the IMF-Dst data sets, the accuracy of the global evolution function for such storms can not be checked readily.

As an example of the prediction of storms, the case of 11 February 1968 is shown in Fig. 1. One-step predictions are obtained at each time t using the known $Dst^*(t)$ and $E_w(t)$ to obtain the predicted $\widetilde{Dst}^*$(t+1) at the following hour, t+1. The result, shown in Fig. 1b, has a mean absolute error of 3.5 nT, averaged over 50 hours. It may be noted that if we assume that $\widetilde{Dst}^*$(t+1) = $Dst^*(t)$ (i.e. persistence) the one step mean absolute error is about 5 nT for this storm. Iterated predictions starting at time t+1 can be made by using $Dst^*(t)$ and $E_w(t)$ at time t, and E_w at the subsequent time steps, t+1, t+2, t+3, etc. This yields an iterated prediction in which the predicted $\widetilde{Dst}^*$(t+1) and $E_w(t+1)$ are used to obtain $\widetilde{Dst}^*$(t+2) at the next time step, and so on. The iterated prediction for 50 hours is shown in Fig. 1c and has a mean absolute error of 10 nT. The forecasting ability of this model, Eq.(2), is assessed by obtaining the best model parameters using all but one of the 14 storms and then predicting the remaining one. To compare these out-of-sample predictions, the iterations are started 10 hours before the storm peak. A mean absolute prediction error is computed from the beginning of the prediction to 10 hours after the storm peak, so that the results are not affected by the recovery phase. For the 14 storms this yielded

mean absolute errors between 5 and 25 nT with a median of 15 nT.

3. Local Input–Output Model

A more general description of the solar wind - magnetosphere interaction can be obtained by constructing the phase space of magnetospheric dynamics on the storm time scales using the method of time delay embedding adapted to input-output systems [*Casdagli*, 1992] as has been done for the AL index [*Price et al.*, 1994; *Vassiliadis et al.*, 1995]. An input–output phase space is reconstructed by taking the normalized dusk-dawn electric field E_w as the input and Dst^* as the output. The trajectory in the phase space is represented by the time evolution of the state vector $\vec{X}(t) = [Dst^*(t), Dst^*(t-\tau_{out}), ...; E_w(t), E_w(t-\tau_{in}), ...]$. For the storms in the OMNI database the choice $\vec{X}(t) = [Dst^*(t), E_w(t)]$ is adequate in most cases.

In this reconstructed phase space the predicted value $\widetilde{Dst}^*$ (t+1) is given in Eq.(1) where the functional F is obtained by a linear Taylor expansion around $\vec{X}(t)$ and the coefficients are computed by a fitting procedure that uses the evolution of the nearest neighbors of $\vec{X}(t)$ [*Farmer et al.*, 1987]. This model can describe complex functions by adjusting itself to the different conditions of the solar wind - magnetosphere system. For the case shown in Fig. 1b the number of nearest neighbors was fixed at 5. This one-step prediction can be used to yield an iterated prediction for many time steps by using $\widetilde{Dst}^*$ (t+1) to define $\vec{X}(t+1)$ and to obtain a new set of nearest neighbors, and so on. This local linear procedure is used to make out-of-sample predictions by reconstructing the phase space with all storms except the one to be predicted. Iterated predictions starting 10 hours before the storm peak to 10 hours after the storm peak were made for the 14 cases, and the mean absolute errors ranged between 5 to 25 nT, with a median of 12 nT.

The prediction for the magnetic storm of 11 February 1968 is shown in Fig. 1. The middle panel (Fig.1b) shows a sequence of one step (1 hour) predictions with a mean absolute error of 4.5 nT, which in this case is higher than the mean absolute error for the global model. The lower panel (Fig. 1c) shows the iterated prediction which tracks the overall evolution of the storm, with an excellent agreement during the critical main phase but is not as good in the recovery phase for this particular case, although the mean absolute error is only 20 nT. These errors show that the procedure can predict accurately the storm development using the local phase space structure.

4. Modeling Storms from Dst Data

The input - output approach is successful in predicting and describing quantitatively the storm onset and evolution, but it requires the solar wind data for hours

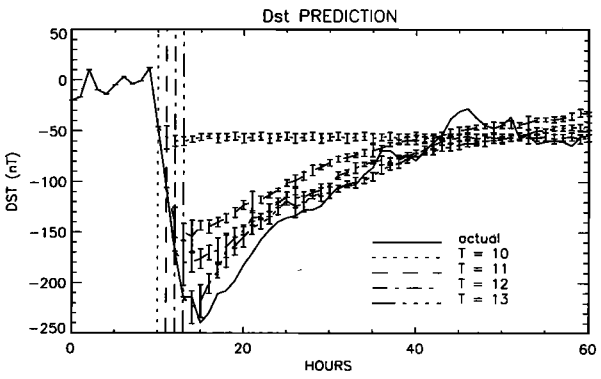

Figure 2. Autonomous prediction procedure for the storm of 19 December 1980. The solid curve is the actual storm, and the predictions generated every hour beginning with t = 10 are shown. The vertical lines show the beginning of the predictions. At t =12 the convergence of the predictions is clear and thus the storm is well predicted. The vertical error bars represent the averaged absolute prediction error of the nearest neighbors using the same local linear model.

in advance. Furthermore, continuous solar wind data for storm occurrences is very sparse (only 14 cases in the OMNI database). It is therefore natural to investigate the predictability of storms from Dst alone.

We consider a phase space in which the state of the system at a given time is represented by $\vec{X}(t) = [Dst(t), Dst(t-1)]$ and evolves according to Eq.(1) where the local functional F, reconstructed as above, represents patterns in the Dst which are used to predict its subsequent evolution. In the absence of the solar wind input the storm onset can not be predicted and the attempt is to describe quantitatively the subsequent evolution of a storm that has reached a threshold value, e.g., -50 nT. Iterated 50 hour out-of-sample predictions are updated every time step (1 hr), thus giving a sequence of iterated predictions as shown in Fig. 2 for the storm of 19 December 1980. The first iterated prediction is made at t = 10 where $Dst \simeq -50$ nT and subsequent iterated predictions are made starting at t = 11, t = 12 and t = 13. The mean absolute errors with respect to the actual Dst averaged over 30 hours are 81, 37, 20 and 13 nT, respectively. From the forecasting point of view, the actual Dst is not known and a measure of the forecast accuracy is the convergence of the sequence of forecasts in time. A measure of the convergence between the iterated predictions generated from time t_2, $\{Dst^{(t_2)}(t_2+T) : T = 0, 1, ..., 30\}$, and the iterated predictions generated from the previous time $t_1 = t_2$-1, $\{Dst^{(t_1)}(t_1+1+T) : T = 0, 1, ..., 30\}$, is

$$d(t_2) = \frac{1}{30}\sum_{T=0}^{30} |Dst^{(t_2)}(t_2+T) - Dst^{(t_1)}(t_2+T)| \quad (3)$$

and has the values 45, 19 and 12 nT for $t_2 = 11$, 12 and 13, respectively. This clearly indicates the convergence of the sequence of iterated predictions. An important

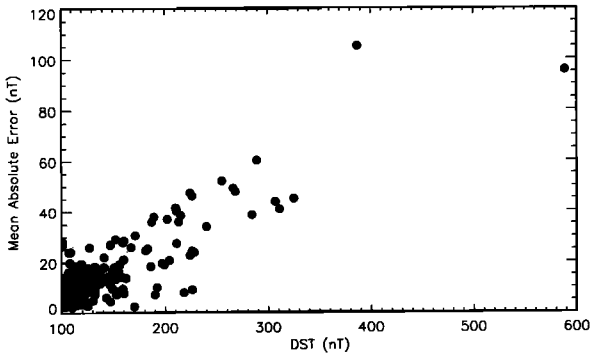

Figure 3. The mean absolute errors of the autonomous (only Dst data used) iterated predictions are plotted as a function of storm magnitudes. The prediction are started when the Dst goes below -75 nT.

feature of these predictions is their ability to forecast the peak and recovery phase as the storm progresses (Fig. 2), thus predicting when the worst of the storm will be over.

To quantify statistically the effectiveness of predicting the evolution of a storm using autonomous (Dst alone) iterated prediction, another threshold value of -75 nT was chosen to start out-of-sample iterated predictions for the 140 cases with Dst < -100 nT from the OMNI database. The iterated predictions were carried only 10 hours past the minimum of the Dst to avoid contamination from the recovery phase. The mean absolute errors of the iterated predictions increase with Dst magnitude, as shown in Fig. 3. It is clear that the evolution of storms with $Dst > -300$ nT can be predicted well with this procedure. The average error is however significantly higher for big and rare storms ($Dst < -350$ nT), due in some degree to the lack of data on these infrequent events. This fact itself can be used as a forecasting tool. If the sequence of predictions converges (i.e. d(t) defined by Eq.(3) decreases as t increases), the forecasts are convergent and thus reliable. On the other hand, if these predictions fail to converge as the storm intensifies, the algorithm is unable to develop a good model due mainly to the lack of similar events in the data base. Thus the storm in progress is likely to be a large storm with peak Dst value below -350 nT (see Fig. 3), for which the available data is very sparse. In other words, the lack of convergence in the predictions is a strong indication that the storm in progress will reach Dst below -350 nT. Based on the statistics of the predictions shown in Fig. 3 this can be used as a warning for a severe storm.

5. Conclusions

The solar wind - ring current interaction during intense magnetic storms has been modeled as an input-output system, reconstructed from the Dst and solar wind data, as a closed-form global differential equation (1) and by a more general local linear evolution model, yielding good predictions of the storm onset and its evolution. Other forms of the nonlinear functional F were used without significant improvement. The model based on the Dst time series alone is capable of predicting the evolution of a storm in progress. These nonlinear techniques can be used as a forecasting tool for space weather in two ways: (1) the input-output models if solar wind parameters are available, (2) local prediction of a storm in progress if solar wind parameters are absent. The two methods can be combined into a single practical tool for predicting magnetic storms, using solar wind data when available and Dst data otherwise.

Acknowledgments. This research was supported by NSF grant ATM-9211883 and NASA grants NAGW-3596 and NAG5-1101. We wish to thank T. Detman for many critical and useful comments.

References

Brown R., Rulkov N. F., Tracy E. R., Modeling and synchronizing chaotic systems from time series data, *Phys. Rev. E, 49* 3784, 1994

Burton R. K., R. L. McPherron, and C. T. Russell, An empirical relationship between interplanetary conditions and Dst, J. Geophys. Res., 80, 4204, 1975.

Casdagli M., A dynamical system approach to modeling input-output systems, in *Nonlinear modeling and forecasting*, edited by M. Casdagli and S. Eubanks, pp. 265-282, Addison-Wesley, Reading, Mass., 1992.

Farmer J.D. and J.J. Sidorowich, Predicting chaotic time series, *Phys. Rev. Lett., 59*, 845, 1987.

Gonzalez W. D., J. A. Joselyn, Y. Kamide, H. W. Kroehl, G. Rostoker, B. T. Tsurutani, V. M. Vasyliunas, What is a Manetic Storm? J. Geophys. Res., 99, 5771, 1994.

Joselyn J. A., Geomagnetic activity forecasting: The state of the art, *Rev. Geophys., 33*, 3, August 1995.

Price C. P., D. Prichard, and J. E. Bischoff, Nonlinear input-output analysis of auroral electrojet index, J. Geophys. Res., 99, 13227, 1994.

Sharma A. S., Assessing the nonlinear behavior of the magnetosphere: Its dimension is low, its predictability is high (US National Report to IUGG, 1991-1994), *Rev. Geophys., 33*, 645 (Supple.), 1995.

Vassiliadis D., Klimas A. J., Baker D. N. Roberts D. A., A description of the solar wind-magnetosphere coupling based on nonlinear prediction filters, J. Geophys. Res., 100, 3495, 1995.

J. A. Valdivia, A. S. Sharma, K. Papadopoulos, Dept. of Physics, Dept. of Astronomy, University of Maryland, College Park, MD 20742 (e-mail: alejo@spp.astro.umd.edu; ssh@spp.astro.umd.edu; kp@spp.astro.umd.edu)

(Received March 6, 1996; revised August 2, 1996; accepted September 3, 1996.)